Medical University of Graz | Otto Loewi Research Center

Fred Hutch Cancer Center

Marshall Plan Scholarship

Final report

Localization & composition of lymphoid aggregates in NSCLC

Research fellowship
Fred Hutch Cancer Center

Ana Santiso

25.07.22-25.03.2023

supervision by

Dr. McGarry Houghton, M.D.

Clinical Research Division,

Fred Hutch Cancer Center, Seattle, WA, USA

1. Abstract

The presence of tumor-infiltrating B-cells, intratumoral immunoglobins and tertiary lymphoid structures (TLS) correlate with survival of patients presenting several types of solid tumors, including NSCLC. However, anti- and pro-tumorigenic functions have been linked to B-cells present in the tumor microenvironment (TME).The specific phenotype and function of B cells present in a tumor at a given time might ultimately depend on the specific cellular and signaling context within the TME. Seeing that understanding pro- and anti-tumor B-cell phenotypes could be key to modulating B-cell responses in the TME towards anti-tumor immunity, it is of high importance to determine the characteristics and function of specific B cell subpopulations present in the tumors of NSCLC patients. In order to characterize B-cells and their roles in the TME, it is not enough to define the phenotype of specific subsets. It is also necessary to put them into context by analyzing their spatial and temporal distribution within the tumor. Looking at how these subsets cluster within the TME and their proximity to other immune cell types might provide key information regarding their functionality and roles in cancer development.Overall, exploring how these subsets cluster within the TME and their proximity to other immune cell types might provide key information regarding their functionality and roles in cancer development.

Table of Contents

2. List of abbreviations

AB	antibody
APC	antigen opresenctiong cell
FDC	follicular dendritic cell
GC	germinal center
HEV	high endothelial venule
LA	lymphoid aggregate
$LT\alpha_1\beta_2$	lymphotoxin-$\alpha_1\beta_2$
nfLAs	non follicular lymphoid aggregates
NSCLC	non small cell lung cancer
ROI	region of interest
SLO	secondary lymphoid organ
TLS	teriary lymphoid structure
TME	tumor micro environment

3. Introduction

3.1. B cells in cancer

In the past few years, several studies have been published on how the presence of tumor-infiltrating B-cells and intra-tumoral immunoglobins correlate with survival of patients with several types of cancer, including NSCLC.(1–5) However, their potential as immunotherapy target or as biomarkers, is still largely unclear.

Overall in cancer, a wide range of anti-tumorigenic as well as pro-tumorigenic functions have been linked to B-cells present in the tumor microenvironment (TME).(6) The tumor suppressing roles ascribed to tumor infiltrating B cells include standard B-cell functions such as the secretion of immunoglobins against tumor antigens.(7–9) Production of these antibodies in the TME can lead to opsonization and the antibody dependent killing of cancer cells via cytotoxicity. (10) These lymphocytes also promote the anti-tumoral T-cell response in their role as antigen presenting cells (APCs)(11,12). A B-cell subset has also been described, that has the capacity to promote cytotoxic T-cell survival and proliferation in antigen independent manner, mainly through CD27/CD70 interactions.(13) Furthermore, a less prominent feature of B cells is that they can directly lyse tumor cells by producing Granzyme B, TRAIL and IFNγ. (14,15)

Notably, B cells play a crucial role in tertiary lymphoid structures (TLS). On the one hand, they help maintain TLS structure via the secretion of chemokines and cytokines such as CXCL13(16) and lymphotoxin-$\alpha_1\beta_2$ ($LT\alpha_1\beta_2$).(17) They also participate in the germinal center (GC) reaction that takes place within mature TLS. These ectopic lymphoid organs that develop in non-lymphoid tissues at sites of chronic inflammation like tumors, display a similar structural organization to that of secondary lymphoid organs (SLOs). Their presence can exacerbate the local immune response, as antigen-specific T- and B-cells can undergo terminal differentiation into effector cells within them. It has been shown that their presence correlates with better patient outcome in many solid tumor cancer types.(18) B cell and B-cell related signaling pathways may therefor play a key role in the activation of the anti-tumorigenic immune response through humoral immunity and local immune activation via TLS. (19)

Evidence has also been reported for pro-tumorigenic functions of B-cells. Regulatory B-cells and immunosuppressive plasma cells express factors such as the immunosuppressive cytokines IL-10, TGF-α, as wells as other factors, like PD-L1, IL-35 and Tim-1, which all can contribute to an immunosuppressive TME. (20,21) B-cells have also been shown to activate the local compliment system (via activation of complement system components C5a or C3a), which induces tumor-promoting inflammation and angiogenesis.(22) Whether B-cells adopt a pro- or anti-tumorigenic phenotype might ultimately depend on the specific cellular and signaling context within the TME.

3.2. Lymphoid aggregates

Lymphoid aggregates (LAs) are dense structures of immune cells that can be found in non-lymphoid tissues. They arise in conditions of chronic inflammation, such as cancer. (19) There are several different types of LAs. They differ from each other in cellular composition, structure and in some cases their location. Based on current knowledge, aggregates found in tumors can be classified into two main groups: non follicular aggregates and TLSs. A short overview of the different types of LAs as described in literature can be found in Figure 1. In a recent review by Laumont et. al. (2022), Laumont and colleagues proposed further possible categorizations for LAs. The review not only describes the different possible classification groups for these structures, but also highlights the knowledge gaps in our current understanding of them. (23)

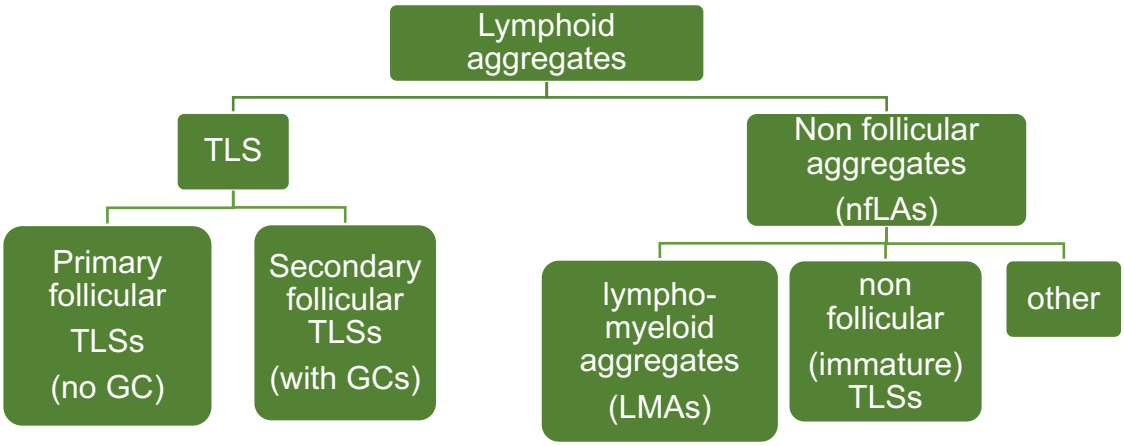

Figure 1- *Types of lymphoid aggregates present in tumors.*

In NSCLC patients, LAs can be found within the tumor stroma, at the tumor border and even in adjacent normal lung tissue. Among the different types of aggregates, TLSs are the best characterized. These structures resemble the follicles of secondary lymphoid organs (SLOs). Evidence suggests that the primary functions of TLSs are fulfilled in their germinal centers and that they are analogue to those in SLOs. Mainly the priming of antigen specific T cells and the mounting of ectopic GC reactions that lead to the rise of antigen producing Plasmacells(9,10) and memory B cells(24). In the context of cancer, TLSs arise de novo (via lymphoid neogenesis) in response to antigens and inflammatory stimuli. (25–27)

According to Laumont et. al, there are two main types of TLSs: primary follicular TLSs and secondary follicular TLSs. For a LA to be considered a primary follicular TLS, it must have (at minimum) clearly demarcated B cell follicles containing $CD21^{+}$ follicular dendritic cells (FDCs) and adjacent T cell zones containing conventional dendritic cells and high endothelial venules (HEVs). Primary follicular TLSs mature into secondary follicular TLSs and can be identified because they contain GCs.(28) Figure 2 presents with a schematic representation of a secondary follicular TLS, its components and general organization. There is a wide number of markers across the literature that

have been used to identify and characterize the cellular components of TLSs. Table 1 summarizes the main markers that have been used to characterize TLSs via immunostaining.

It should be noted that even though TLSs bear major resemblance to SLOs, they present with some differences. For instance, in contrast to SLOs, TLSs lack a capsule.(29) Laumont et. al propose that this likely results in greater exposure to immunoregulatory factors and apoptotic and/or necrotic debris from the TME. Also, TLSs lack subcapsular sinus macrophages, which have been shown to play an integral role in antigen presentation to B cells in lymph nodes. Finally, tumor- associated GCs typically lack well- defined dark and light zones (28)

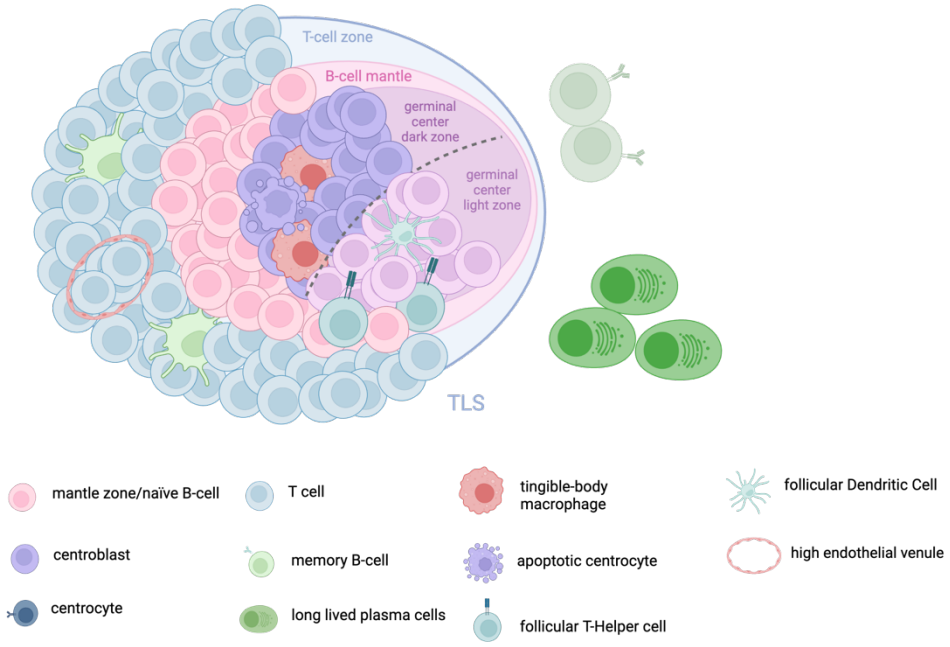

Figure 2- *schematic representation of a secondary follicular TLS. The graphic shows the most common cellular components, as well as their localization within the structure. Figure generated via Biorender.*

Non follicular aggregates (nf-LAs) are a less well-defined group. Laumont et. al proposed various possible subcategories of these aggregates, however very little is known about their functional status. LAs that fall into this category may include, among others, forms of TLS that have no discernable structure because of their maturation state. In addition, there are aggregates that may be defined by their myeloid cell content. Laumont coined the term lympho-myeloid aggregates to refer to this group and pointed out that it may include further subcategories of LAs that functionally differ from each other. However, what all LAs have in common, is that they are highly dense agglomerations of immune cells that contain large amounts of T and B cells.

Table 1- *Published markers for the characterization of TLSs*

Protein marker	Immune cell type	References
CD20	B cells	(3,5,30–33)
CD79A	B cells	(2,9,34)
CD23	follicular B cells follicular DCs	(3,5,7,10,35,36)
Bcl6	GC B cells	(7,10,36,37)
IgD	naïve B cells mantle zone B cells	(7,38,39)
IgM	B cells	(39,40)
IgG	B cells	(40)
AID	GC B cells	(7,9)
CD10	GC Bcells	(41)
CD3	T cells	(3–5,9,10,25,34,35,37,38,42)
CD4	T helper cells	(5,39,39,40)
CD8	Cytotoxic T cells	(4,5,35,39)
DC-Lamp	Mature DCs	(7,36,43)
CD21	Follicular DCs	(5,9,23,25,28,35–37,39–41,44)
CD35	Follicular DCs	(39)
CD68	(tingible body) macrophages	(23,39,45)
Ki67	Proliferating cells	(4,7,37,39)
PNAD	HEV	(3,9,10,25,28,36,37,43,46,47)
CXCR5	Follicular Th cells (T_{hf})	(3,4,10,38,40,48)
CXCL13	T_{hf}	(40,49,50)
PD1	T_{hf}	(40,49)

3.3. Hypothesis and aims

The primary aim of the research stay was to get training in the implementation of the multiplex immunofluorescence platform Vectra®. This imaging system allows for simultaneous antibody-based detection and quantification of the expression of up to seven markers and a nuclear counterstain on a single tissue section. The method has also been proven to be reliable for the detection of co-expression of tumor biomarkers. Based on the principle of sequential cycles where individual epitopes are labelled with antibodies, followed by enzymatic detection, the Houghton lab has established and published several protocols for up to seven simultaneous markers. A further goal of the project was to put together, optimize & apply to a cohort of patient samples two 7-plex mIF-Panels designed for the detection of B cells and tertiary lymphoid structures (TLSs). During the research stay, I not only learned to perform the staining and imaging of patient sample slides, I was also trained on the use of the image analysis HALO® from indica labs. HALO® is currently the gold standard image analysis platform for quantitative tissue analysis in digital pathology. I used the software to analyze the composition of lymphoid aggregates. I not only analyzed the images that resulted from the staining of my designed panels, I also analyzed images from a third panel that had been previously stained at the Houghton lab. The most important data analysis goals for my research stay can be summarized as follows:

1. **Identify lymphoid aggregates (LAs) in both the tumor and lung area of sample slides and quantify LA abundance and area.**

2. **Determine composition of LAs and the maturation status of TLSs.**

3. **Spatially determine the expression of selected, validated exploratory markers on B-cells in LAs of tumor and lung.**

Finally, I had the opportunity during my research stay to be introduced to the CODEX (co-detection by indexing) imaging platform. This is a high-throughput, MIF technology that can be used to detect more than 40 biomarkers simultaneously in a single tissue sample. It can also be used to assess the relative abundance and expression of biomarkers at a spatial level. The technology is based on antibodies conjugated to barcodes comprised of unique oligonucleotide sequences, making the detection highly specific. Although the focus of my project was on the Vectra platform, I had the opportunity to learn about the CODEX and its current implementations at the Fred Hutch Cancer Center from the experts that are currently establishing and implementing this technology for various projects.

4. Materials and Methods

4.1. Multiplex Immunofluorescence- Opal™ immunohistochemistry

Deparaffinization

Sample slides cut from FFPE blocks were baked at 56°C for one hour. After cooldown (10 min or aver night), the slides were rehydrated by dipping them in Xylene (3 times 7 min), 100% EtOH (2 times 2 min) 95% EtOH (2 times 2 min), 70% EtOH (1 time 2 min) and dd$H_2$0 (1 time 2 min) consecutively. The slides were then kept in fresh ddH_2O until the first antigen retrieval step of the staining.

Staining

A total of two panels were designed and used for staining of patient sample slides. Deparaffinized slides were stained for 7 markers in a cyclic manner using the PerkinElmer Opal™ 7-color IHC Kit. Each cycle started with an antigen retrieval step at 98°C (steaming). In the first cycle, this step was performed using Trilogy™ buffer (cell marque). Subsequent antigen retrievals were performed using AR6 buffer (Perkin Elmer). After antigen retrieval, endogenous peroxidases were blocked by incubating the slides in 3% H_2O_2 for 10 min. Following peroxidase inactivation, non-specific antibody (AB) binding sites were blocked using TCT buffer (TBS+ 0.25% bovine casein) for 30 min. Unlabeled primary antibodies were diluted to previously determined optimal concentrations and incubated on slides for one hour. The concentration and clone of each antibody can be found in tables 2 and 3. The “Opal Polymer HRP Mouse and rabbit” reagent was used as secondary antibody reagent and slides were incubated with it for 20 min after each primary antibody binding. Markers were then detected using the Opal™ detection substrate in a 1:80 dilution. The designated fluorophore for each marker can be found in tables 2 and 3. Washing steps were performed using TBS-T buffer.

Scanning

Multispectral imaging of the stained slides was executed using the Vectra® 3 quantitative pathology imaging System from Akoya Biosciences. Scanning protocols were set up and included optimized exposure times for each filter cube (DAPI, FITC, Cy3, Texas Red and Cy5) and magnification used during image acquisition. After performing a whole slide scan (10x), regions of interest (ROIs) were marked using the Phenochart™ software (AKOYA Bioscience). ROIs were then rescanned at 20x magnification. The acquired ROI images were processed for signal unmixing using the inForm® tissue finder with MOTiF™ software. (Version 2.6). The images were spectrally unmixed using previously established spectral libraries.

Image Analysis

Image analysis of unmixed ROI images was performed using HALO®. Images were annotated and positive cells gated by threshold. Analysis was performed for a total of three panels. Apart from the B cell and TLS panel, the ROIs of a third panel were annotated for LAs and their composition analyzed. The markers that were included into this panel can be found in table 3. The antibody composition of this panel has been published before (Kargl et.al, 2019) and can be found in the publication. (51)

***Table 2**-primary antibodies, B cell panel (Panel1)*

Marker	CD70	Bcl6	CD55	CD20	CD138	CK
Primary AB clone	E3Q1A	E5I8I	E7G2U	L26	IHC138	AE1/AE3
Primary AB concentration (µg/ml)	0.6	0.125	0.43	0.21	0.07	0.42
Primary AB vendor & catalogue number	Cell Signaling 69209S	Cell Signaling 89369S	Cell Signaling 31759S	Dako GA604	Cell Signaling 30501S	Dako M3515
Opal™ reagent	Opal620	Opal650	Opal570	Opal520	Opal690	Opal540

***Table 3-**primary antibodies, TLS panel (Panel 2)*

Marker	CXCR5	Bcl6	CD4	CD68	CD20	CK
Primary AB clone	D6L3C	E5I8I	EP204	PG-M1	L26	AE1/AE3
Primary AB concentration (µg/ml)	0.0025	0.125	0.00825	0.2	0.21	0.42
Primary AB vendor & catalogue number	Cell Signaling 72172S	Cell Signaling 89369S	Millipore Sigma 104R-24	Dako M0876	Dako GA604	Dako M3515
Opal™ reagent	Opal690	Opal650	Opal570	Opal620	Opal520	Opal540

Table 4- *Myeloid cell and CD8+ T cell panel (Panel 3)*

Marker	Cell type
CD8	Cytotoxic T cells
HLA-DR	APCs
CD68	Macrophages
CD66b	Neutrophils
CK	Tumor/cells
CD14	Monocytes

4.2. Patient cohort

Patient samples were selected from a cohort of patients whose TME had been previously analyzed via flow cytometry by Kargl et.al (2019) These patients had been classified into four immune subtypes depending on the immune composition of their TME. For this study, patients form two of these subgroups (active and myeloid) were selected. Patients from the active group were classified as such because their TME was characterized by a robust $CD8^+$ T cell infiltration. Patients of the myeloid group on the other hand presented with sparse T cell infiltration and an abundant myeloid cell content. (51) The number of slides stained for each panel can be found in Table 4.

Table 5*-stained slides*

Immune status	Panel	Number of stained slides
Active	B cells	15
	TLSs	6
Myeloid	B cells	16
	TLSs	6

4.3. Data analysis

Analysis for the B cell and TLS panel (Panels 1&2) is ongoing. Resulting data is planned to be included in a publication and cannot be disclosed within this report. Information provided in this section applies to the analysis of tumor slides stained with Panel 3, which identified macrophages, neutrophils, APCs, monocytes, MDSCs and cytotoxic T cells.

Identification of lymphoid aggregates

In HALO® lymphoid aggregates were annotated according to their density (visually recognized). Potential false annotations were excluded based on the method proposed by Barmpoutis et. al. for the identification of aggregates based on their density. (52) For this analysis, a cutoff was introduced for densities below one standard deviation from the median. Annotated aggregates with a total cell density below cutoff were excluded from further analysis.

Identification of TLS

TLSs were identified according to their structure and the expression of HLADR and CD68 in the follicular area.

Identification of immune cell populations

Immune cell populations were identified according to their individual marker expression. The analysis algorithm in HALO® was programmed to discriminate cell identity not only by fluorescence signal threshold but by percentage of membrane positive for a given marker.

Tabulation, plotting and statistical analysis

Data extracted from HALO® was analyzed in R Version 4.2.2. The applied statistical test was paired Wilcoxon-signed-rank test. Statistical outliers were identified and removed by applying the IQR method. The Ggplot package version 3.4.2 was used to create plots.

5. Results

After visual recognition and annotation, the identity of lymphoid aggregates was corroborated according to their cell density. TLSs were identified by a central area containing HLADR$^+$ cells colocalized with CD68$^+$ macrophages. This central area was surrounded by an area containing CD8$^+$ T cells. (Figure 3D & 3E). Non follicular aggregates were identified solely on their cell density. (Figure 3F). The mean density of lymphoid aggregates (0.01284 cells/µm²) was 1.89 times higher than the median density of the stroma (0.0069 cells/µm²). (Figure 3G) Visually annotated lymphoid aggregates that had a density beneath 1 standard deviation of the mean were excluded from further analysis to avoid misidentification. (Figure 3A) A total of 392 nfLAs (219 in the active group, 173 in the myeloid group) and 13 TLS (12 in the active group and 1 in the myeloid group) were identified according to these criteria. There was no significant difference in median total cell density of LAs between tumors of different histology. The median total cell density of the structures was comparable also in tumors with different immune subtypes (active vs. myeloid). (Figure 3B & 3C).

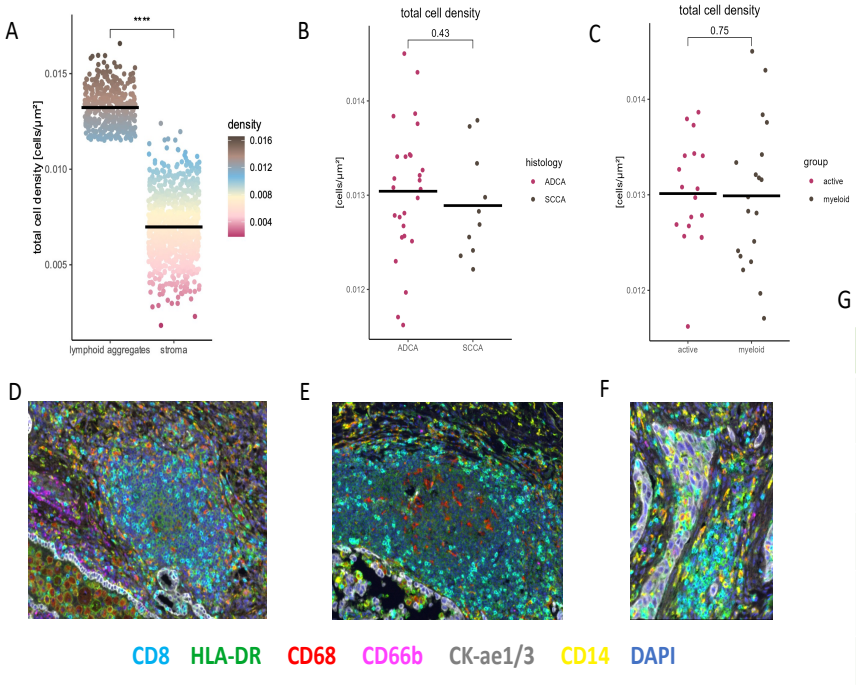

	ICP2 cohort Active + myeloid groups
cell number	min= 51 max= 6249 mean = 512
LA area	min= 3663.54 µm² max= 449267.4 µm² mean=39141.9 µm²
cell density in LAs	mean= 0,013225 cells/µm² SD= 0,0013 cells /µm²
celll density stroma	Mean=0,007 cells/µm² SD= 0,0017 cells/µm²
LA: stroma density ratio	1,89

***Figure 3**-Identified lymphoid aggregates on slides stained with Panel 3. The slides of X patients was annotated for LAs. Visually annotated lymphoid aggregates that had a density beneath 1 SD of the median were excluded from further analysis. For comparisons between groups, the medians for total cell densities of LAs were calculated for each patient. (A) total cell density of identified lymphoid aggregates and the corresponding stroma. (B) Comparison of median cell densities between histologies ADCA (n=) and SCCA (n=). (C) Comparison of median cell densities between patients with an active TME and a myeloid TME. (D-F) Representative images for LA organizational types, the identified markers and their corresponding colors. D and E show TLSs, while F shows a non-follicular lymphoid aggregate.*

Identified aggregates with a density higher than the set cut-off (0,0132 cells/µm² and higher) were analyzed for their cellular composition. Cytotoxic T cells ($CD8^+$), neutrophils ($CD66^+$), MDSCs ($CD14^+CD68^-HLADR^-$), monocytes ($CD14^+$ $CD68^-$ $HLA\text{-}DR^+$), macrophages ($CD68^+CD14^{-/+}$ $HLADR^{-/+}$), and other APCs ($HLADR^+$ $CD8^-$ $CD14^-$ $CD68^-$) were identified via HALO analysis. The median density of the different cell types in LAs was calculated for each patient. A comparison of the median densities between the two immune groups showed no significant differences between the myeloid and active groups. (Figure 4) However, there were trends showing that the LA of patients with a myeloid TME presented a higher density of APCs (figure 4F), macrophages (figure 4G), and neutrophils (figure 4A). These LAs also tended to have a lower density of $CD8^+$ T cells (figure 4E). A comparison for macrophage subtypes (figure 5) showed that there is a significant difference in median density for ($CD68^+$) $CD14^+$ $HLADR^+$ macrophages (figure 5A), ($CD68^+$) $CD14^+$ $HLADR^-$ macrophages (figure 5B), and ($CD68^+$) $CD14^-$ $HLADR^+$ macrophages (Figure 5C).

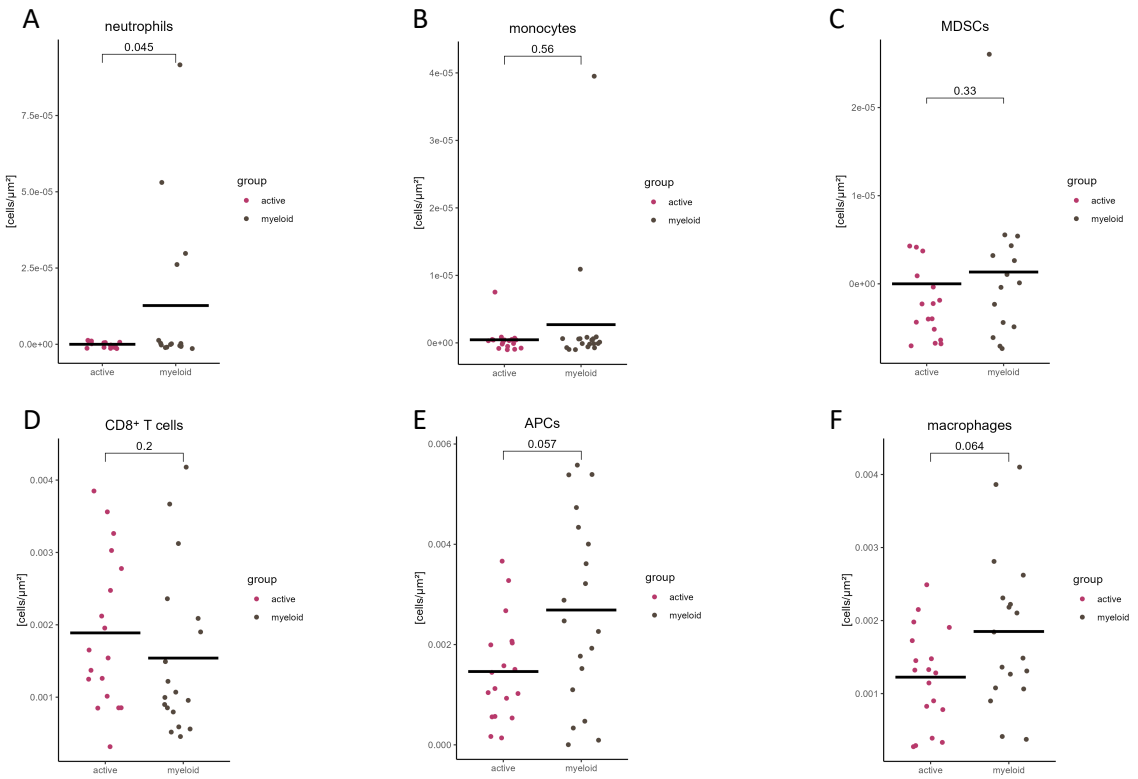

Figure 4*-Comparisons for median cell density between patients with active and myeloid TME for identified immune cell groups. (A) Median neutrophil density (cells/ µm²) in lymphoid aggregates of patients of the active and myeloid group. (B) Median monocyte density (cells/ µm²) in lymphoid aggregates of patients of the active and myeloid group. (C) Median MDSC density (cells/ µm²) in lymphoid aggregates of patients of the active and myeloid group. (D) Median $CD8^+$ T cells density (cells/ µm²) in lymphoid aggregates of patients of the active and myeloid group. (E) Median APCs density (cells/ µm²) in lymphoid aggregates of patients of the active and myeloid group. (E) Median macrophage density (cells/ µm²) in lymphoid aggregates of patients of the active and myeloid group.*

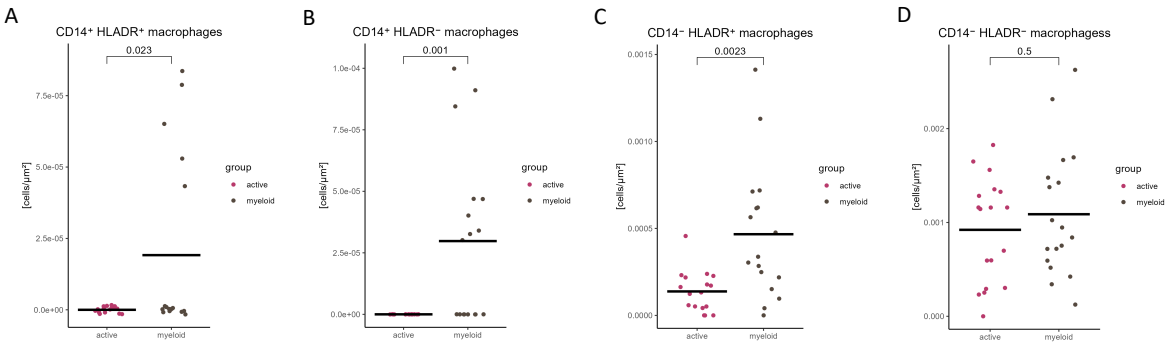

Figure 5*-Comparisons for median cell density between patients with active and myeloid TME for identified immune cell groups. (A) Median CD14⁺ HLADR⁺ macrophage density (cells/ µm²) in lymphoid aggregates of patients of the active and myeloid group. (B) Median CD14⁺ HLADR⁻ macrophage density (cells/ µm²) in lymphoid aggregates of patients of the active and myeloid group. (C) Median CD14⁻ HLADR⁺ macrophage density (cells/ µm²) in lymphoid aggregates of patients of the active and myeloid group. (C) Median CD14⁻ HLADR⁻ macrophage density (cells/ µm²) in lymphoid aggregates of patients of the active and myeloid group.*

6. Discussion

Panel 3 contained none of the markers traditionally used for LA and or/TLS identification, we were able to successfully identify LAs based on their cellular density. The resulting parameters for the annotated LAs (max and min density, area and LA: stroma ratio) were comparable with those published by Barmpoutis et. al. Specially when taking into consideration the fact that we used total cell densities instead of lymphocyte cells densities for the identification of aggregates. By introducing a cut off for any visually annotated aggregates with a density below one SD of the mean, we insured that any aggregates with densities comparable to those of the stroma were excluded from further analysis.

TLSs were easily identified visually. Their appearance and marker expression were in line with what has been previously described in literature. The central area containing $HLADR^+$ cells colocalized with $CD68^+$ macrophages. The concentrated HLADR signal signifies a large presence of APCs in this area and is in line with the concept of a B cell zone that also contains DCs, follicular DCs and tingilar body macrophages. What is more, $CD8^+$ T cells localized at the periphery of the structures, consistent with the idea of a T-cell zone that surrounds the B cell follicle.

One of the main open questions in the LA field is whether and how the TME affects the formation, maturation, and conformation of LAs. The comparison between patients of different immune groups showed that, while LAs remained independent, definable structures, there were some variations in the immune cell composition between the active and myeloid group. One of the differences was neutrophil content of the LAs. Neutrophils have not been described in literature to be associated to any kind of LA in humans. Nevertheless, HALO® analysis determined neutrophils associated to the identified LAs. There was even a tendency for a higher density of neutrophils in LAs of the myeloid group. Yet, the overall neutrophil density in LAs of either group was extremely low. Taking into consideration that neutrophils were the cellular population most highly associated with the myeloid phenotype(51), this further highlights the accuracy of the LA identification by density.

The difference in the APC and macrophage densities could be of biological relevance and directly linked to the functionality of these structures. On the one hand, antigen presentation is thought to be one of the main functions performed within LAs. It has been described particularly in TLS. However, it is unknown to what extent it plays a role in nfLAs. Our data shows that within LAs of the myeloid group there is a tendency for higher density of APCs when compared to the active group.LAs of the myeloid group also presented significant higher densities of three of the four detected macrophage subtypes. This included both macrophage subtypes that were positive for HLADR. $HLADR^+$ macrophages are generally considered antitumorigenic(53). These macrophages have the potential to engage in antigen presentation. It should be noted though that even though there were significant differences among both $CD14^+$ macrophage subtypes, their density was extremely low in LAs of both the active and myeloid group.

7. Acknowledgements

.

I would like to thank the Austrian Marshall Plan Foundation for the financial support of my research fellowship. The experience not only enabled me to expand my laboratory skills and learn about new and highly valuable methods. It also gave me the opportunity to expand my knowledge in NSCLC and cancer immunology. Greatly contributing to my growth as a researcher.

I would like to acknowledge and thank my supervisor at my home university Dr. Kargl who opened the door for me at my host lab and encouraged me to expand my horizons as a researcher with this stay abroad.

I would also like to express my gratitude Dr. Houghton and the members of his group at the Fred Hutch Cancer Center for having me. I specially would like to thank Dr. Xiaodong Zhu, for not only sharing with me his valuable expertise but also making me feel welcome in Seattle from the beginning of my stay. I greatly appreciated the dedicated time to my project and the many talks about the tumor micro-environment we had. I learned a lot from him, and for that I am very grateful.

8. References

1. Isaeva OI, Sharonov GV, Serebrovskaya EO, Turchaninova MA, Zaretsky AR, Shugay M, et al. Intratumoral immunoglobulin isotypes predict survival in lung adenocarcinoma subtypes. Journal for Immunotherapy of Cancer [Internet]. 2019 [cited 2021 Nov 18];7. Available from: https://www-1ncbi-1nlm-1nih-1gov-10013b5cu071b.han.medunigraz.at/pmc/articles/PMC6819482/

2. Chen J, Tan Y, Sun F, Hou L, Zhang C, Ge T, et al. Single-cell transcriptome and antigen-immunoglobin analysis reveals the diversity of B cells in non-small cell lung cancer. Genome Biology. 2020 Jun 24;21(1):152.

3. Petitprez F, de Reyniès A, Keung EZ, Chen TWW, Sun CM, Calderaro J, et al. B cells are associated with survival and immunotherapy response in sarcoma. Nature. 2020 Jan;577(7791):556–60.

4. Cabrita R, Lauss M, Sanna A, Donia M, Skaarup Larsen M, Mitra S, et al. Tertiary lymphoid structures improve immunotherapy and survival in melanoma. Nature. 2020 Jan;577(7791):561–5.

5. Helmink BA, Reddy SM, Gao J, Zhang S, Basar R, Thakur R, et al. B cells and tertiary lymphoid structures promote immunotherapy response. Nature. 2020 Jan;577(7791):549–55.

6. Fridman WH, Meylan M, Petitprez F, Sun CM, Italiano A, Sautès-Fridman C. B cells and tertiary lymphoid structures as determinants of tumour immune contexture and clinical outcome. Nat Rev Clin Oncol. 2022 Jul;19(7):441–57.

7. Germain C, Gnjatic S, Tamzalit F, Knockaert S, Remark R, Goc J, et al. Presence of B Cells in Tertiary Lymphoid Structures Is Associated with a Protective Immunity in Patients with Lung Cancer. Am J Respir Crit Care Med. 2014 Jan 31;189(7):832–44.

8. Montfort A, Pearce O, Maniati E, Vincent BG, Bixby L, Böhm S, et al. A Strong B-cell Response Is Part of the Immune Landscape in Human High-Grade Serous Ovarian Metastases. Clinical cancer research : an official journal of the American Association for Cancer Research [Internet]. 2017 Jan 1 [cited 2022 Jul 7];23(1). Available from: https://pubmed-1ncbi-1nlm-1nih-1gov-10013b5ki0435.han.medunigraz.at/27354470/?dopt=Abstract

9. Kroeger DR, Milne K, Nelson BH. Tumor-Infiltrating Plasma Cells Are Associated with Tertiary Lymphoid Structures, Cytolytic T-Cell Responses, and Superior Prognosis in Ovarian Cancer. Clinical cancer research : an official journal of the American Association for Cancer Research [Internet]. 2016 Jun 15 [cited 2022 Jul 9];22(12). Available from: https://pubmed-1ncbi-1nlm-1nih-1gov-10013b50g012c.han.medunigraz.at/26763251/?dopt=Abstract

10. Meylan M, Petitprez F, Becht E, Bougoüin A, Pupier G, Calvez A, et al. Tertiary lymphoid structures generate and propagate anti-tumor antibody-producing plasma cells in renal cell cancer. Immunity. 2022 Mar 8;55(3):527-541.e5.

11. Bruno TC, Ebner PJ, Moore BL, Squalls OG, Waugh KA, Eruslanov E, et al. Antigen-Presenting Intratumoral B Cells Affect CD4 + TIL Phenotypes in Non-Small Cell Lung Cancer Patients. Cancer immunology research [Internet]. 2017 Oct [cited 2021 Nov 18];5(10). Available from: https://pubmed-1ncbi-1nlm-1nih-1gov-10013b5cu071b.han.medunigraz.at/28848053/?dopt=Abstract

12. Wennhold K, Thelen M, Lehmann J, Schran S, Preugszat E, Garcia-Marquez M, et al. CD86 + Antigen-Presenting B Cells Are Increased in Cancer, Localize in Tertiary Lymphoid Structures, and Induce Specific T-cell Responses. Cancer immunology research [Internet]. 2021 Sep [cited 2022 Jul 9];9(9). Available from: https://pubmed-1ncbi-1nlm-1nih-1gov-10013b50g012c.han.medunigraz.at/34155067/?dopt=Abstract

13. Deola S, Panelli MC, Maric D, Selleri S, Dmitrieva, Voss CY, et al. Helper B cells promote cytotoxic T cell survival and proliferation independently of antigen presentation through CD27/CD70 interactions. Journal of immunology (Baltimore, Md : 1950) [Internet]. 2008 Feb 1 [cited 2021 Oct 2];180(3). Available from: https://pubmed-1ncbi-1nlm-1nih-1gov-10013b5pe0158.han.medunigraz.at/18209030/

14. Leong TL, Bryant VL. B cells in lung cancer-not just a bystander cell: a literature review. Translational lung cancer research [Internet]. 2021 Jun [cited 2022 Jul 10];10(6). Available from: https://pubmed-1ncbi-1nlm-1nih-1gov-10013b50g012c.han.medunigraz.at/34295681/

15. Patel AJ, Richter A, Drayson MT, Middleton GW. The role of B lymphocytes in the immuno-biology of non-small-cell lung cancer. Cancer Immunol Immunother. 2020 Mar;69(3):325–42.

16. Litsiou E, Semitekolou M, Galani IE, Morianos I, Tsoutsa A, Kara P, et al. CXCL13 production in B cells via Toll-like receptor/lymphotoxin receptor signaling is involved in lymphoid neogenesis in chronic obstructive pulmonary disease. Am J Respir Crit Care Med. 2013 Jun 1;187(11):1194–202.

17. Myers RC, King RG, Carter RH, Justement LB. Lymphotoxin α1β2 expression on B cells is required for follicular dendritic cell activation during the germinal center response. European journal of immunology [Internet]. 2013 Feb [cited 2022 Jul 10];43(2). Available from: https://pubmed-1ncbi-1nlm-1nih-1gov-10013b50g012c.han.medunigraz.at/23112125/

18. Sautès-Fridman C, Petitprez F, Calderaro J, Fridman WH. Tertiary lymphoid structures in the era of cancer immunotherapy. Nat Rev Cancer. 2019 Jun;19(6):307–25.

19. Schumacher TN, Thommen DS. Tertiary lymphoid structures in cancer. Science (New York, NY) [Internet]. 2022 Jan 7 [cited 2022 Jul 10];375(6576). Available from: https://pubmed-1ncbi-1nlm-1nih-1gov-10013b50g012c.han.medunigraz.at/34990248/

20. Inoue S, Leitner WW, Golding B, Scott D. Inhibitory effects of B cells on antitumor immunity. Cancer research [Internet]. 2006 Aug 1 [cited 2022 Jul 10];66(15).

Available from: https://pubmed-1ncbi-1nlm-1nih-1gov-10013b50g012c.han.medunigraz.at/16885377/?dopt=Abstract

21. Schwartz M, Zhang Y, Rosenblatt JD. B cell regulation of the anti-tumor response and role in carcinogenesis. Journal for immunotherapy of cancer [Internet]. 2016 Jul 19 [cited 2022 Jul 10];4. Available from: https://pubmed-1ncbi-1nlm-1nih-1gov-10013b50g012c.han.medunigraz.at/27437104/

22. Roumenina LT, Daugan MV, Noé R, Petitprez F, Vano YA, Sanchez-Salas R, et al. Tumor Cells Hijack Macrophage-Produced Complement C1q to Promote Tumor Growth. Cancer immunology research [Internet]. 2019 Jul [cited 2022 Jul 9];7(7). Available from: https://pubmed-1ncbi-1nlm-1nih-1gov-10013b50g012c.han.medunigraz.at/31164356/?dopt=Abstract

23. Laumont CM, Banville AC, Gilardi M, Hollern DP, Nelson BH. Tumour-infiltrating B cells: immunological mechanisms, clinical impact and therapeutic opportunities. Nature reviews Cancer [Internet]. 2022 Jul [cited 2022 Jul 12];22(7). Available from: https://pubmed-1ncbi-1nlm-1nih-1gov-10013b50g0537.han.medunigraz.at/35393541/

24. Weisel FJ, Zuccarino-Catania GV, Chikina M, Shlomchik MJ. A Temporal Switch in the Germinal Center Determines Differential Output of Memory B and Plasma Cells. Immunity. 2016 Jan 19;44(1):116–30.

25. Pagliarulo F, Cheng PF, Brugger L, van Dijk N, van den Heijden M, Levesque MP, et al. Molecular, Immunological, and Clinical Features Associated With Lymphoid Neogenesis in Muscle Invasive Bladder Cancer. Front Immunol. 2021;12:793992.

26. Kang W, Feng Z, Luo J, He Z, Liu J, Wu J, et al. Tertiary Lymphoid Structures in Cancer: The Double-Edged Sword Role in Antitumor Immunity and Potential Therapeutic Induction Strategies. Front Immunol [Internet]. 2021 [cited 2022 Jul 10];0. Available from: https://www-1frontiersin-1org-10013b50g012c.han.medunigraz.at/articles/10.3389/fimmu.2021.689270/full

27. Ukita M, Hamanishi J, Yoshitomi H, Yamanoi K, Takamatsu S, Ueda A, et al. CXCL13-producing CD4+ T cells accumulate in the early phase of tertiary lymphoid structures in ovarian cancer. JCI Insight. 2022 Jun 22;7(12):e157215.

28. Laumont CM, Nelson BH. B cells in the tumor microenvironment: Multi-faceted organizers, regulators, and effectors of anti-tumor immunity. Cancer Cell. 2023 Mar 13;41(3):466–89.

29. Pimenta EM, Barnes BJ. Role of Tertiary Lymphoid Structures (TLS) in Anti-Tumor Immunity: Potential Tumor-Induced Cytokines/Chemokines that Regulate TLS Formation in Epithelial-Derived Cancers. Cancers (Basel). 2014 Apr 23;6(2):969–97.

30. Wu Z, Zhou J, Xiao Y, Ming J, Zhou J, Dong F, et al. CD20 + CD22 + ADAM28 + B Cells in Tertiary Lymphoid Structures Promote Immunotherapy Response. Frontiers in immunology [Internet]. 2022 May 11 [cited 2022 Jul 12];13. Available

from: https://pubmed-1ncbi-1nlm-1nih-1gov-10013b50g0537.han.medunigraz.at/35634306/

31. Shi JY, Gao Q, Wang ZC, Zhou J, Wang XY, Min ZH, et al. Margin-Infiltrating CD20+ B Cells Display an Atypical Memory Phenotype and Correlate with Favorable Prognosis in Hepatocellular Carcinoma. Clin Cancer Res. 2013 Nov 1;19(21):5994–6005.

32. Nielsen JS, Sahota RA, Milne K, Kost SE, Nesslinger NJ, Watson PH, et al. CD20+ Tumor-Infiltrating Lymphocytes Have an Atypical CD27− Memory Phenotype and Together with CD8+ T Cells Promote Favorable Prognosis in Ovarian Cancer. Clinical Cancer Research. 2012 Jun 14;18(12):3281–92.

33. Lastwika KJ, Kargl J, Zhang Y, Zhu X, Lo E, Shelley D, et al. Tumor-derived Autoantibodies Identify Malignant Pulmonary Nodules. Am J Respir Crit Care Med. 2019 May 15;199(10):1257–66.

34. Coppola D, Nebozhyn M, Khalil F, Dai H, Yeatman T, Loboda A, et al. Unique Ectopic Lymph Node-Like Structures Present in Human Primary Colorectal Carcinoma Are Identified by Immune Gene Array Profiling. The American Journal of Pathology. 2011 Jul;179(1):37.

35. Vanhersecke L, Brunet M, Guégan JP, Rey C, Bougouin A, Cousin S, et al. Mature tertiary lymphoid structures predict immune checkpoint inhibitor efficacy in solid tumors independently of PD-L1 expression. Nat Cancer. 2021 Aug;2(8):794–802.

36. Silina K, Soltermann A, Attar FM, Casanova R, Uckeley ZM, Thut H, et al. Germinal Centers Determine the Prognostic Relevance of Tertiary Lymphoid Structures and Are Impaired by Corticosteroids in Lung Squamous Cell Carcinoma. Cancer research [Internet]. 2018 Mar 1 [cited 2022 Jul 12];78(5). Available from: https://pubmed-1ncbi-1nlm-1nih-1gov-10013b50g0537.han.medunigraz.at/29279354/

37. Gunderson AJ, Rajamanickam V, C C, Bernard B, Pucilowska J, Ballesteros-Merino C, et al. Germinal center reactions in tertiary lymphoid structures associate with neoantigen burden, humoral immunity and long-term survivorship in pancreatic cancer. Oncoimmunology [Internet]. 2021 Mar 17 [cited 2022 Jul 12];10(1). Available from: https://pubmed-1ncbi-1nlm-1nih-1gov-10013b50g0537.han.medunigraz.at/33796412/

38. Shi J, Hou S, Fang Q, Liu X, Liu X, Qi H. PD-1 Controls Follicular T Helper Cell Positioning and Function. Immunity. 2018 Aug 21;49(2):264-274.e4.

39. Garaud S, Buisseret L, Solinas C, Gu-Trantien C, de Wind A, Van den Eynden G, et al. Tumor-infiltrating B cells signal functional humoral immune responses in breast cancer. JCI Insight. 4(18):e129641.

40. Li JP, Wu CY, Chen MY, Liu SX, Yan SM, Kang YF, et al. PD-1+CXCR5−CD4+ Th-CXCL13 cell subset drives B cells into tertiary lymphoid structures of nasopharyngeal carcinoma. J Immunother Cancer. 2021 Jul 12;9(7):e002101.

41. Masuda T, Tanaka N, Takamatsu K, Hakozaki K, Takahashi R, Anno T, et al. Unique characteristics of tertiary lymphoid structures in kidney clear cell carcinoma: prognostic outcome and comparison with bladder cancer. Journal for immunotherapy of cancer [Internet]. 2022 Mar [cited 2022 Jul 12];10(3). Available from: https://pubmed-1ncbi-1nlm-1nih-1gov-10013b50g0537.han.medunigraz.at/35314433/

42. Meylan M, Petitprez F, Lacroix L, Di Tommaso L, Roncalli M, Bougoüin A, et al. Early Hepatic Lesions Display Immature Tertiary Lymphoid Structures and Show Elevated Expression of Immune Inhibitory and Immunosuppressive Molecules. Clin Cancer Res. 2020 Aug 15;26(16):4381–9.

43. Goc J, Germain C, Vo-Bourgais TKD, Lupo A, Klein C, Knockaert S, et al. Dendritic cells in tumor-associated tertiary lymphoid structures signal a Th1 cytotoxic immune contexture and license the positive prognostic value of infiltrating CD8+ T cells. Cancer research [Internet]. 2014 Feb 1 [cited 2022 Aug 1];74(3). Available from: https://pubmed-1ncbi-1nlm-1nih-1gov-10013b5j20043.han.medunigraz.at/24366885/

44. Posch F, Silina K, Leibl S, Mündlein A, Moch H, Siebenhüner A, et al. Maturation of tertiary lymphoid structures and recurrence of stage II and III colorectal cancer. Oncoimmunology. 2018;7(2):e1378844.

45. Kelsen SG, Aksoy MO, Georgy M, Hershman R, Ji R, Li X, et al. Lymphoid follicle cells in chronic obstructive pulmonary disease overexpress the chemokine receptor CXCR3. American journal of respiratory and critical care medicine [Internet]. 2009 May 1 [cited 2022 Aug 1];179(9). Available from: https://pubmed-1ncbi-1nlm-1nih-1gov-10013b55h0008.han.medunigraz.at/19218194/

46. Remark R, Lupo A, Alifano M, Biton J, Ouakrim H, Stefani A, et al. Immune contexture and histological response after neoadjuvant chemotherapy predict clinical outcome of lung cancer patients. Oncoimmunology [Internet]. 2016 Dec 8 [cited 2022 Aug 1];5(12). Available from: https://pubmed-1ncbi-1nlm-1nih-1gov-10013b5j20043.han.medunigraz.at/28123901/

47. Rodriguez AB, Peske JD, Woods AN, Leick KM, Mauldin IS, Meneveau MO, et al. Immune mechanisms orchestrate tertiary lymphoid structures in tumors via cancer-associated fibroblasts. Cell reports [Internet]. 2021 Jul 20 [cited 2022 Jul 30];36(3). Available from: https://pubmed-1ncbi-1nlm-1nih-1gov-10013b5uw00cd.han.medunigraz.at/34289373/

48. Noël G, Fontsa ML, Garaud S, De Silva P, de Wind A, Van den Eynden GG, et al. Functional Th1-oriented T follicular helper cells that infiltrate human breast cancer promote effective adaptive immunity. J Clin Invest. 2021 Oct 1;131(19):e139905.

49. Yang M, Lu J, Zhang G, Wang Y, He M, Xu Q, et al. CXCL13 shapes immunoactive tumor microenvironment and enhances the efficacy of PD-1 checkpoint blockade in high-grade serous ovarian cancer. J Immunother Cancer. 2021 Jan;9(1):e001136.

50. Veatch JR, Lee SM, Shasha C, Singhi N, Szeto JL, Moshiri AS, et al. Neoantigen-specific CD4 + T cells in human melanoma have diverse differentiation states and correlate with CD8 + T cell, macrophage, and B cell function. Cancer cell [Internet]. 2022 Apr 11 [cited 2022 Aug 4];40(4). Available from: https://pubmed-1ncbi-1nlm-1nih-1gov-10013b5t40042.han.medunigraz.at/35413271/

51. Kargl J, Zhu X, Zhang H, Yang GHY, Friesen TJ, Shipley M, et al. Neutrophil content predicts lymphocyte depletion and anti-PD1 treatment failure in NSCLC. JCI Insight. 2019 Dec 19;4(24):e130850, 130850.

52. Barmpoutis P, Di Capite M, Kayhanian H, Waddingham W, Alexander DC, Jansen M, et al. Tertiary lymphoid structures (TLS) identification and density assessment on H&E-stained digital slides of lung cancer. PLoS One. 2021;16(9):e0256907.

53. DeNardo DG, Ruffell B. Macrophages as regulators of tumour immunity and immunotherapy. Nat Rev Immunol. 2019 Jun;19(6):369–82.